ASTROD-GW:

Wei-Tou Ni 倪维斗

National Tsing Hua University

Refs: WTN, ASTROD-GW, IJMPD 25 (2013) 1530006

G. Wang and WTN, Chin. Phys. B (2015) arXiv

A.-M. Wu and WTN, IAA (2015)

WTN, GW detection in space IJMPD 25 (2016) 1530002

Space Detection Band:
LF (100 nHz- 100 mHz) & MF (100 mHz- 10 Hz)

Complete GW Classification

http://astrod.wikispaces.com/file/view/GW-classification.pdf
(MPLA 25 [2010] pp. 922-935; arXiv:1003.3899v1 [astro-ph.CO])

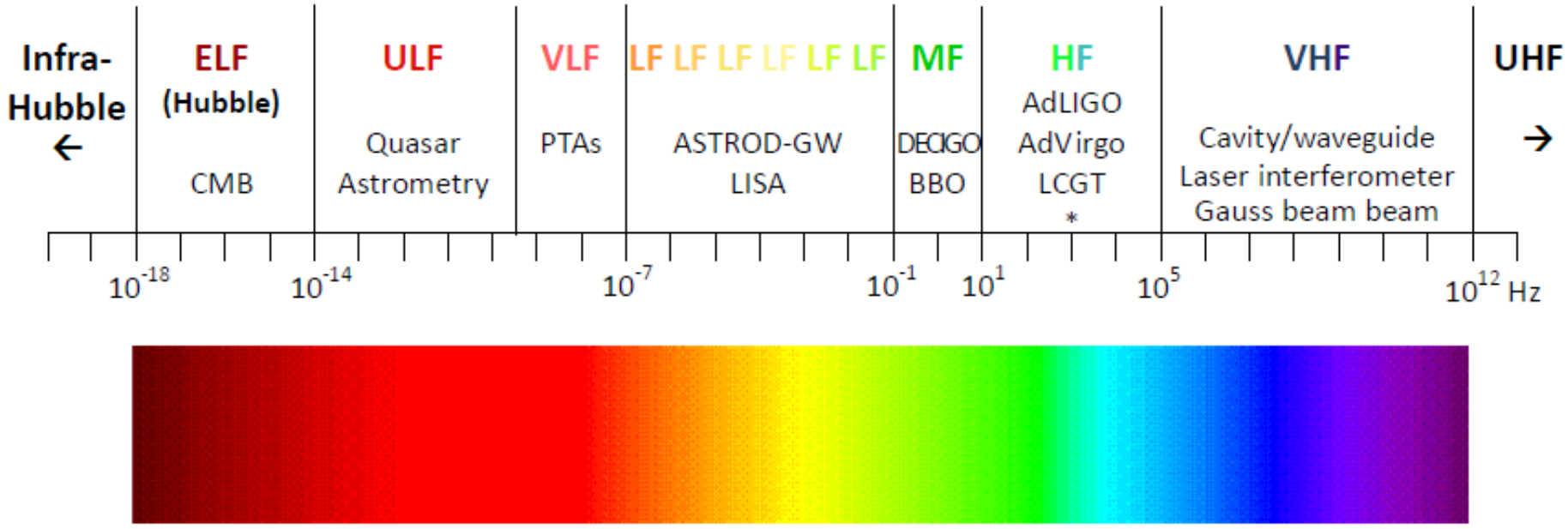

* AIGO, AURIGA, ET, EXPLORER, GEO, NAUTILUS, MiniGRAIL, Schenberg.

Strain power spectral density (psd) amplitude vs. frequency for various GW detectors and GW sources

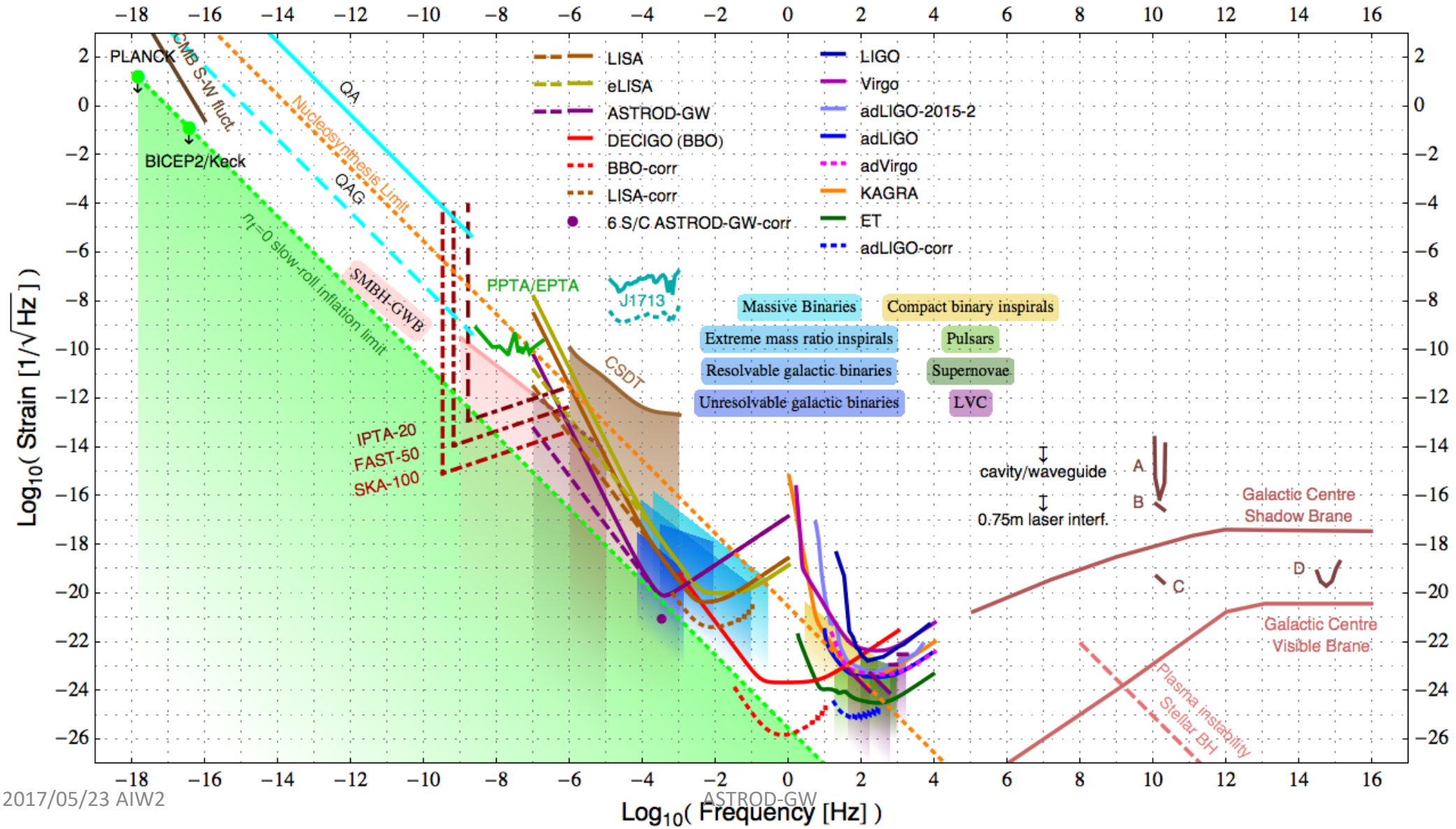

Characteristic strain h_c vs. frequency for various GW detectors and sources. [QA: Quasar Astrometry; QAG: Quasar Astrometry Goal; LVC: LIGO-Virgo Constraints; CSDT: Cassini Spacecraft Doppler Tracking; SMBH-GWB: Supermassive Black Hole-GW Background.]

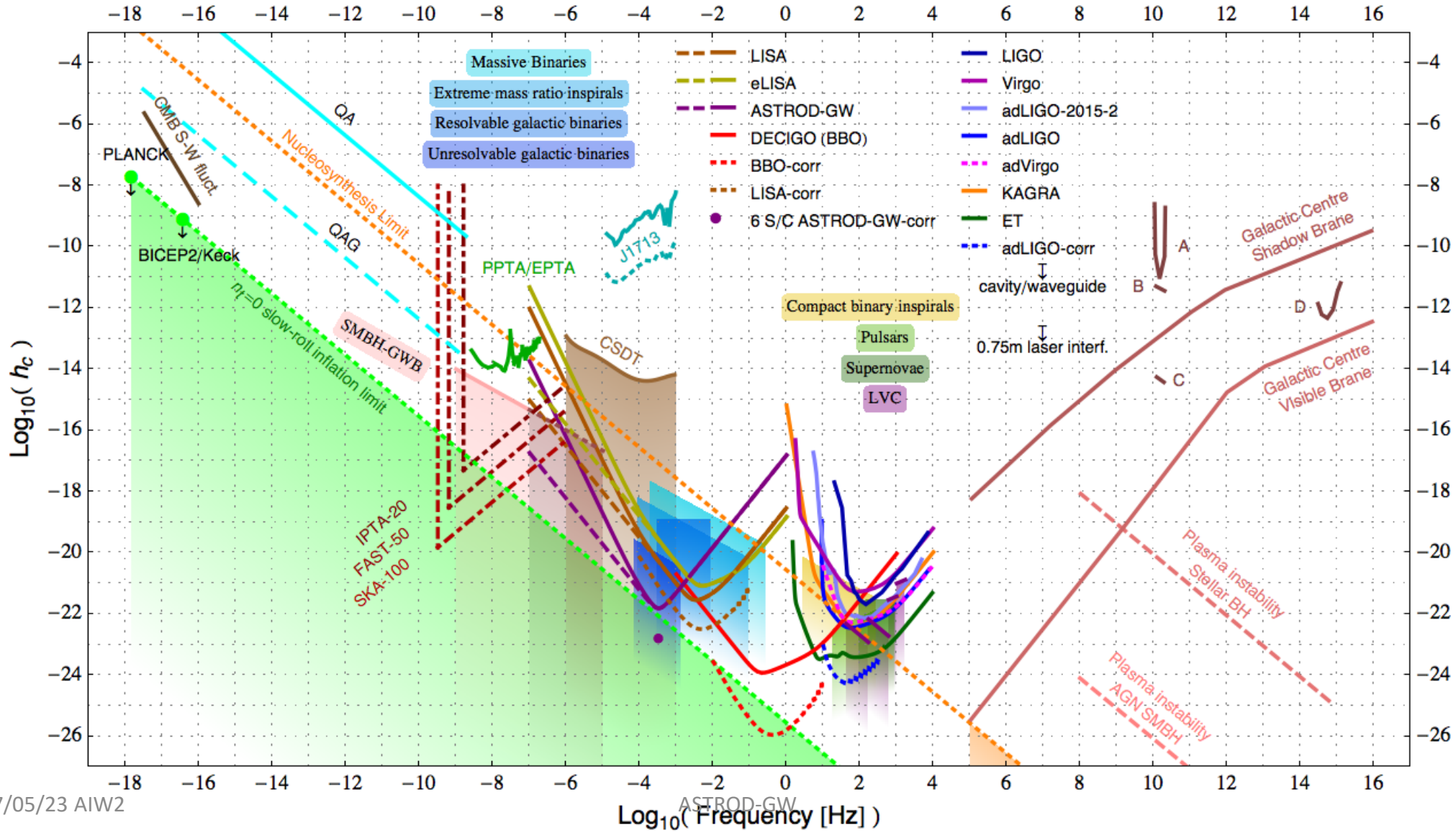

Normalized GW spectral energy density Ω_{gw} vs. frequency for GW detector sensitivities and GW sources

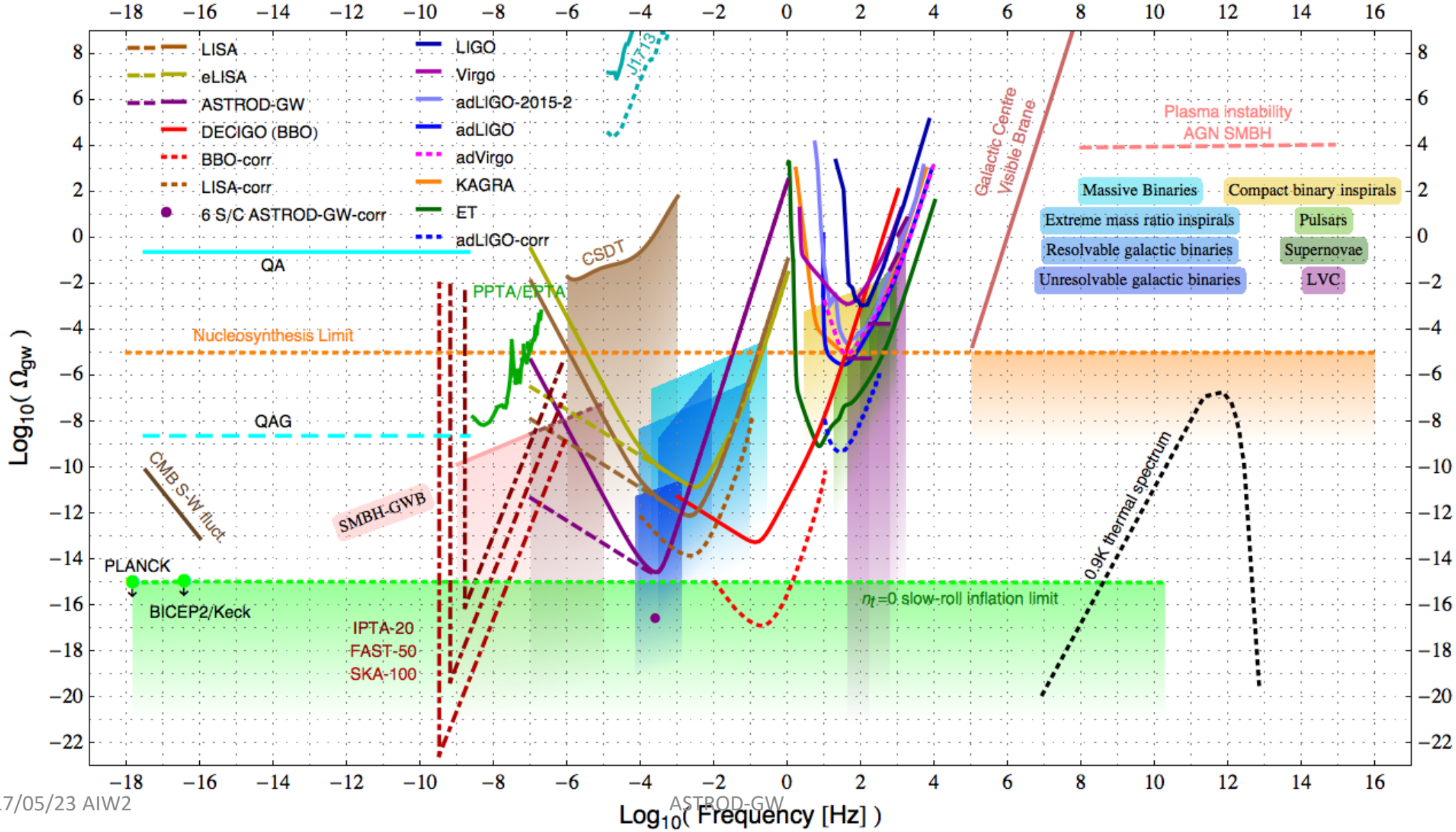

Second Generation GW Mission Concepts

- DECIGO
- BBO
- Super-ASTROD

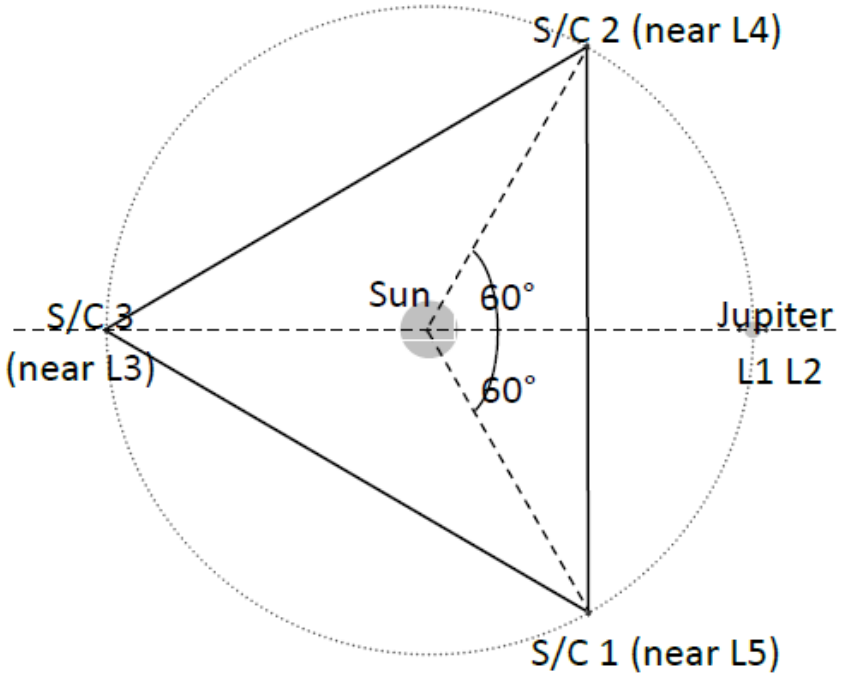

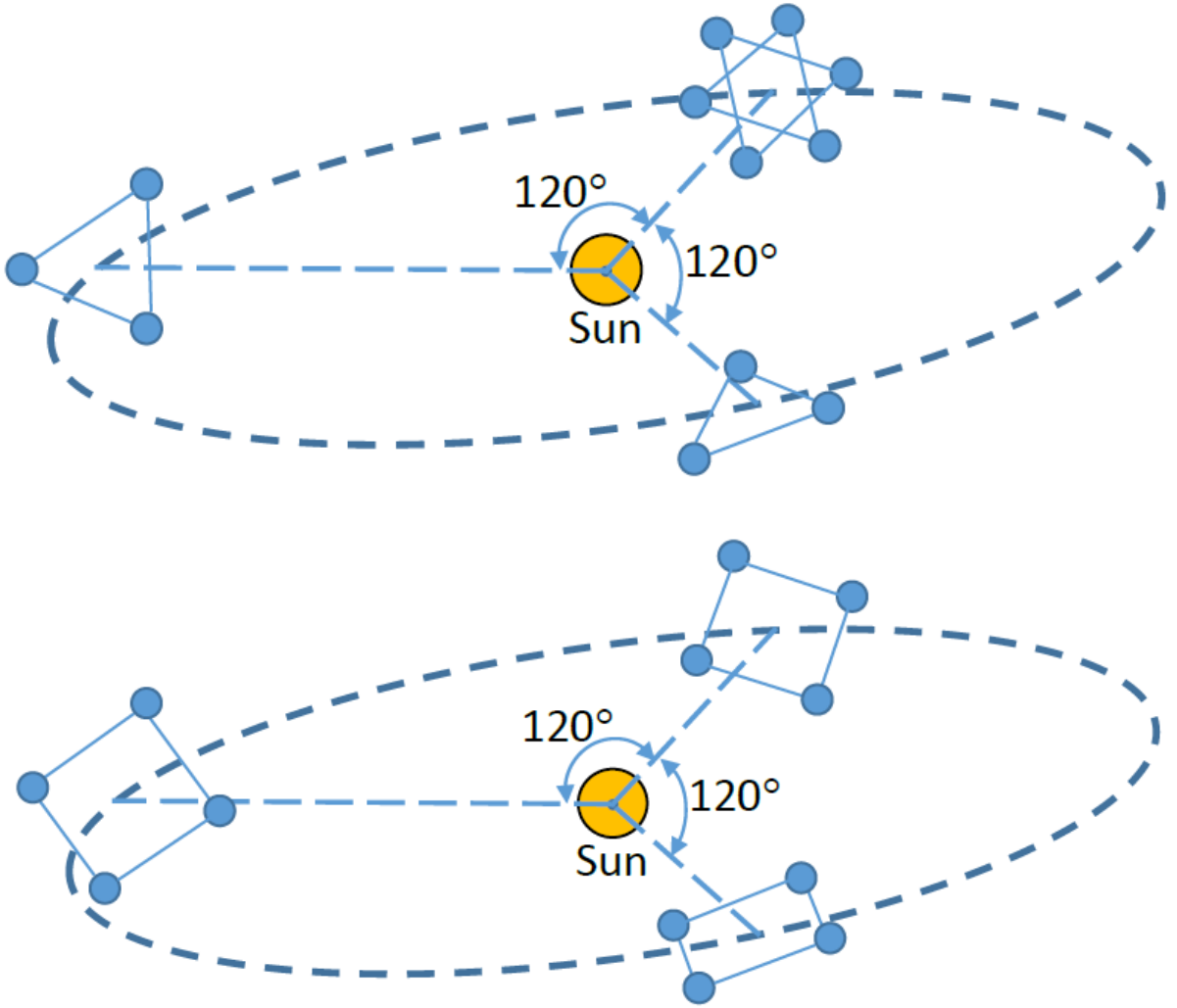

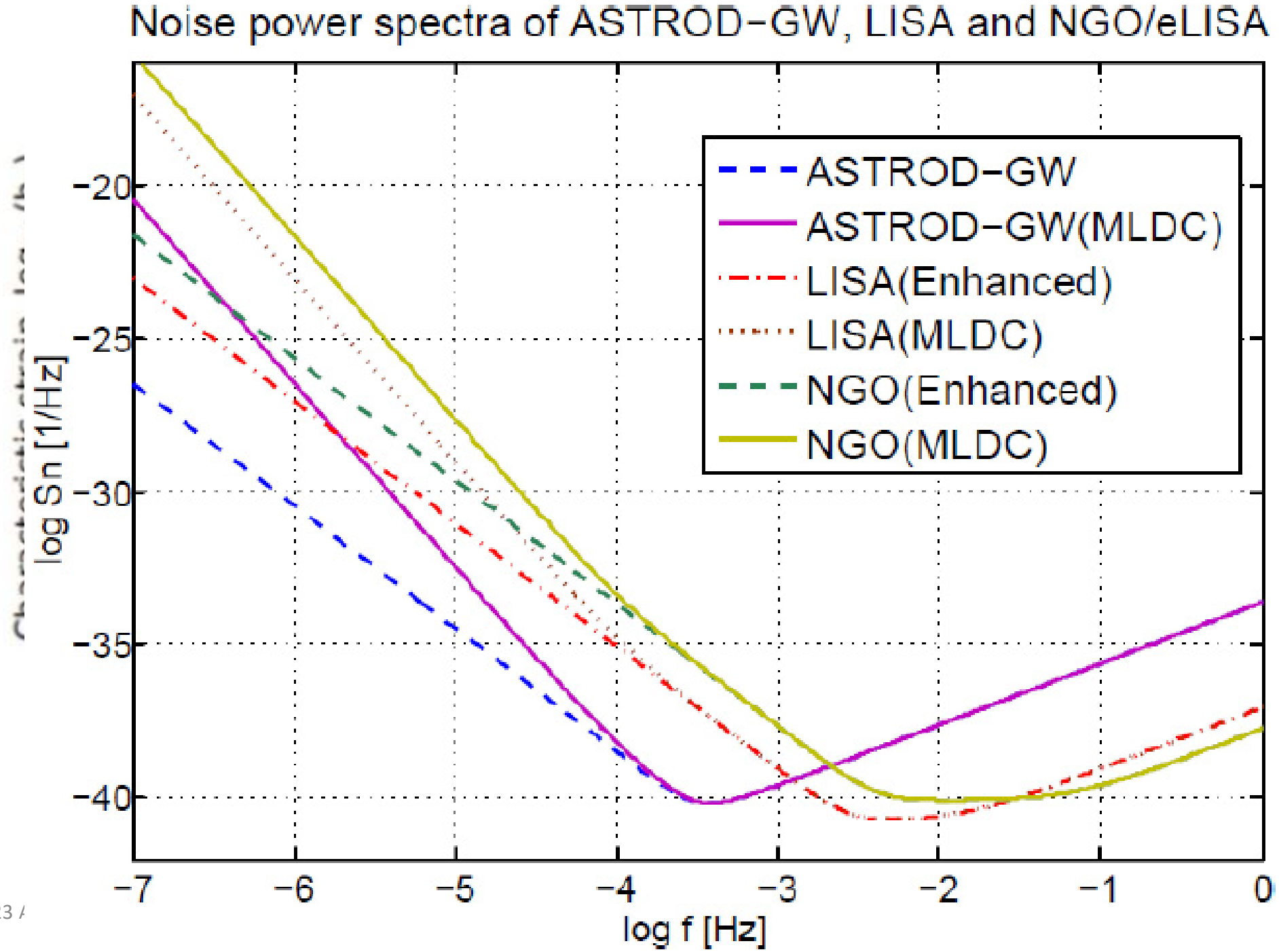
Noise power spectra of ASTROD-GW, LISA and NGO/eLISA
ASTROD-GW
ASTROD-GW(MLDC)
LISA(Enhanced)
LISA(MLDC)
NGO(Enhanced)
NGO(MLDC)
log Sn [1/Hz]
log f [Hz]
−20
−25
−30
−35
−40
−7
−6
−5
−4
−3
−2
−1
0

$$S_{\rm An}^{1/2}(f) = (1/L_{\rm A}) \times \{[(1+0.5(f/f_{\rm A})^2)] \times S_{\rm Ap} + [4S_{\rm a}/(2\pi f)^4]\}^{1/2}\ {\rm Hz}^{-1/2}$$

$$^{\rm (MLDC)}S_{\rm An}^{1/2}(f) = (1/L_{\rm A}) \times \{[(1+0.5(f/f_{A})^2)] \times S_{\rm Ap} + [1+(10^{-4}/f)^2](4S_{\rm a}/(2\pi f)^4)\}^{1/2}\ {\rm Hz}^{-1/2}$$

Strain power spectral density (psd) amplitude vs. frequency for various GW detectors and GW sources. [CSDT: Cassini Spacecraft Doppler Tracking; SMBH-GWB: Supermassive Black Hole-GW Background.]

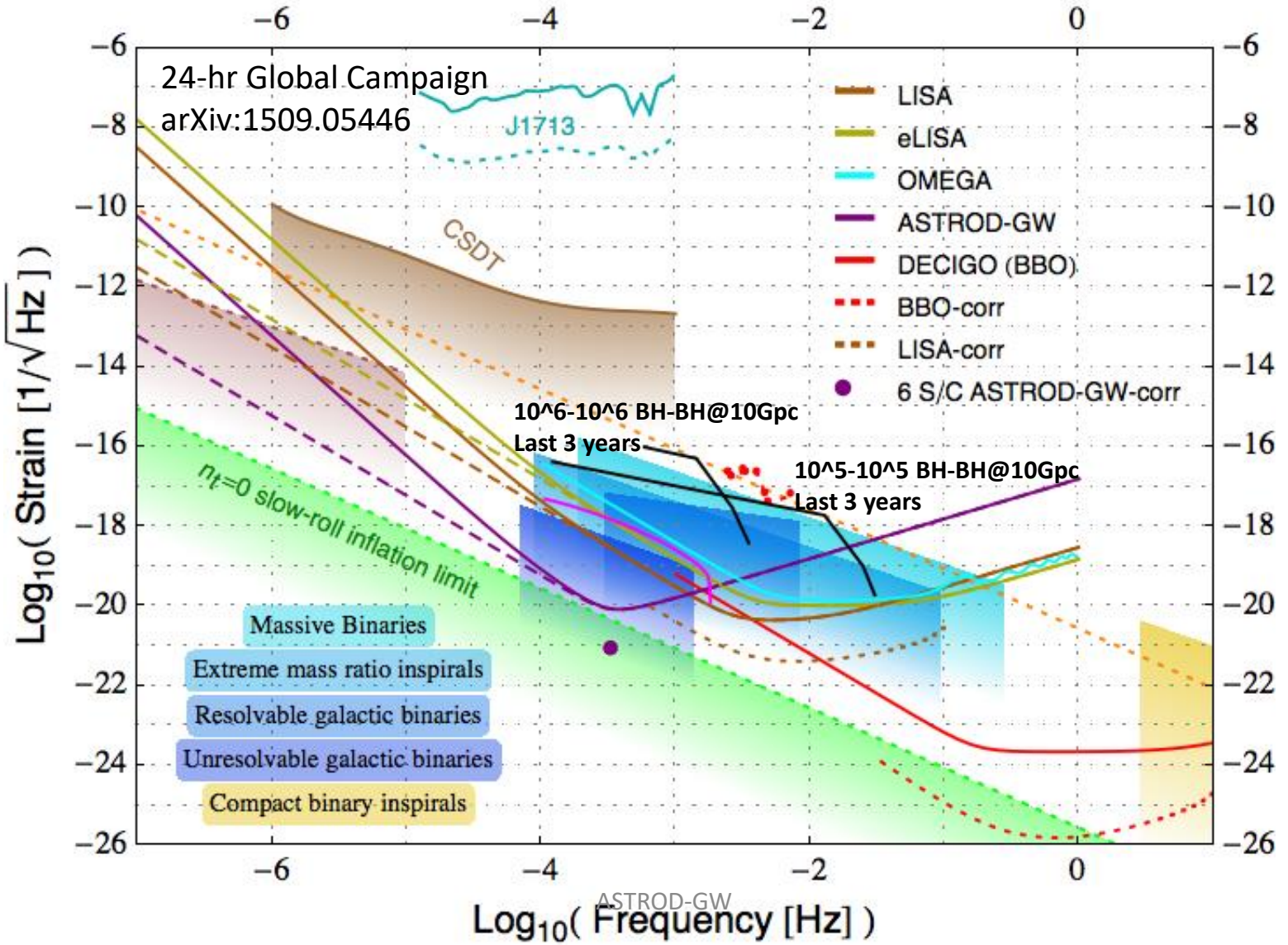

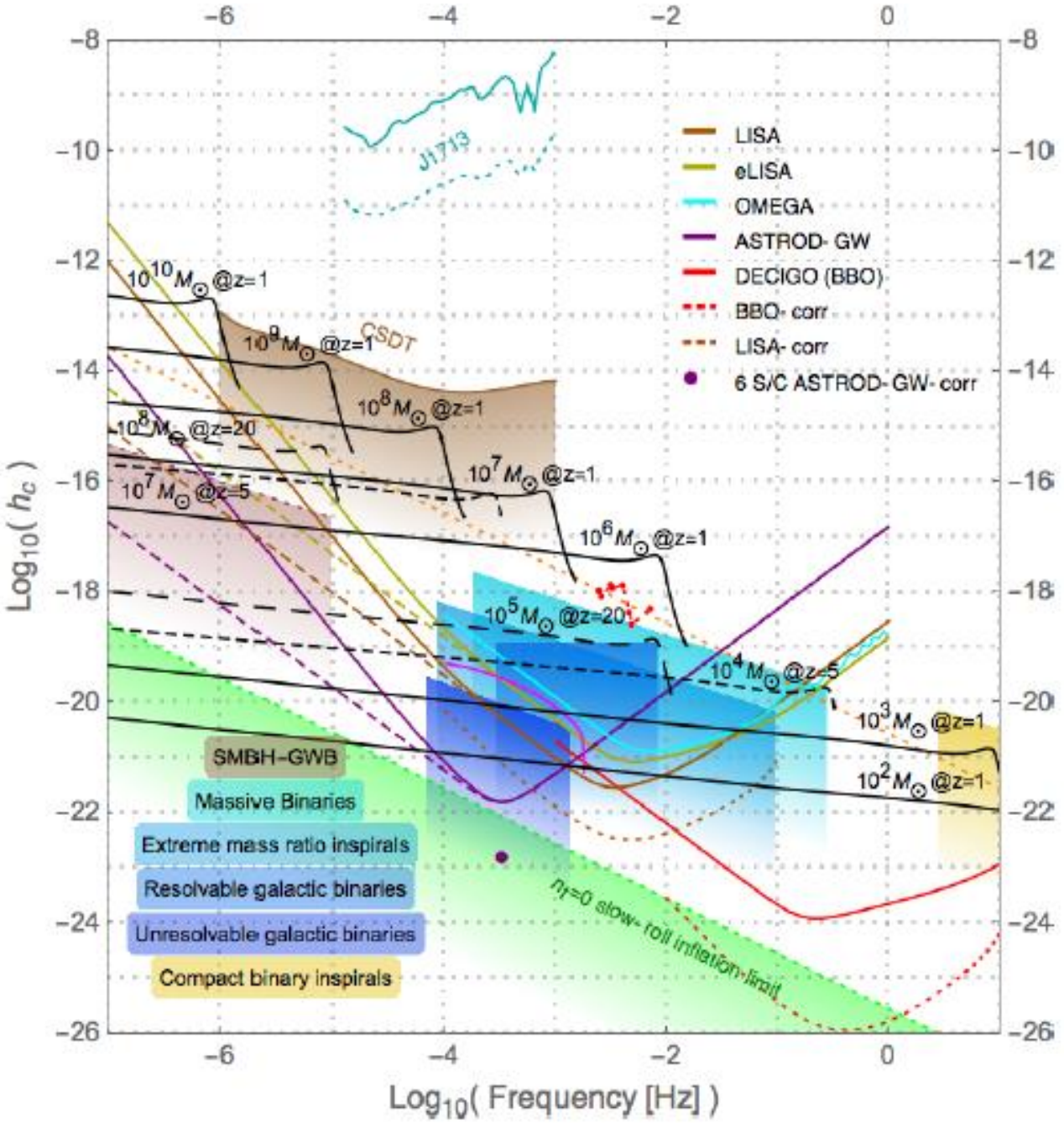
LISA
eLISA
OMEGA
ASTROD- GW
DECIGO (BBO)
BBO- corr
LISA- corr
6 S/C ASTROD- GW- corr
J1713
CSDT
$10^{10}M_\odot$@z=1
$10^{9}M_\odot$@z=1
$10^{8}M_\odot$@z=1
$10^{8}M_\odot$@z=20
$10^{7}M_\odot$@z=1
$10^{7}M_\odot$@z=5
$10^{6}M_\odot$@z=1
$10^{5}M_\odot$@z=20
$10^{4}M_\odot$@z=5
$10^{3}M_\odot$@z=1
$10^{2}M_\odot$@z=1
SMBH-GWB
Massive Binaries
Extreme mass ratio inspirals
Resolvable galactic binaries
Unresolvable galactic binaries
Compact binary inspirals
n_t=0 slow- roll inflation limit
$\mathrm{Log}_{10}(h_c)$
Log_{10}(Frequency [Hz])

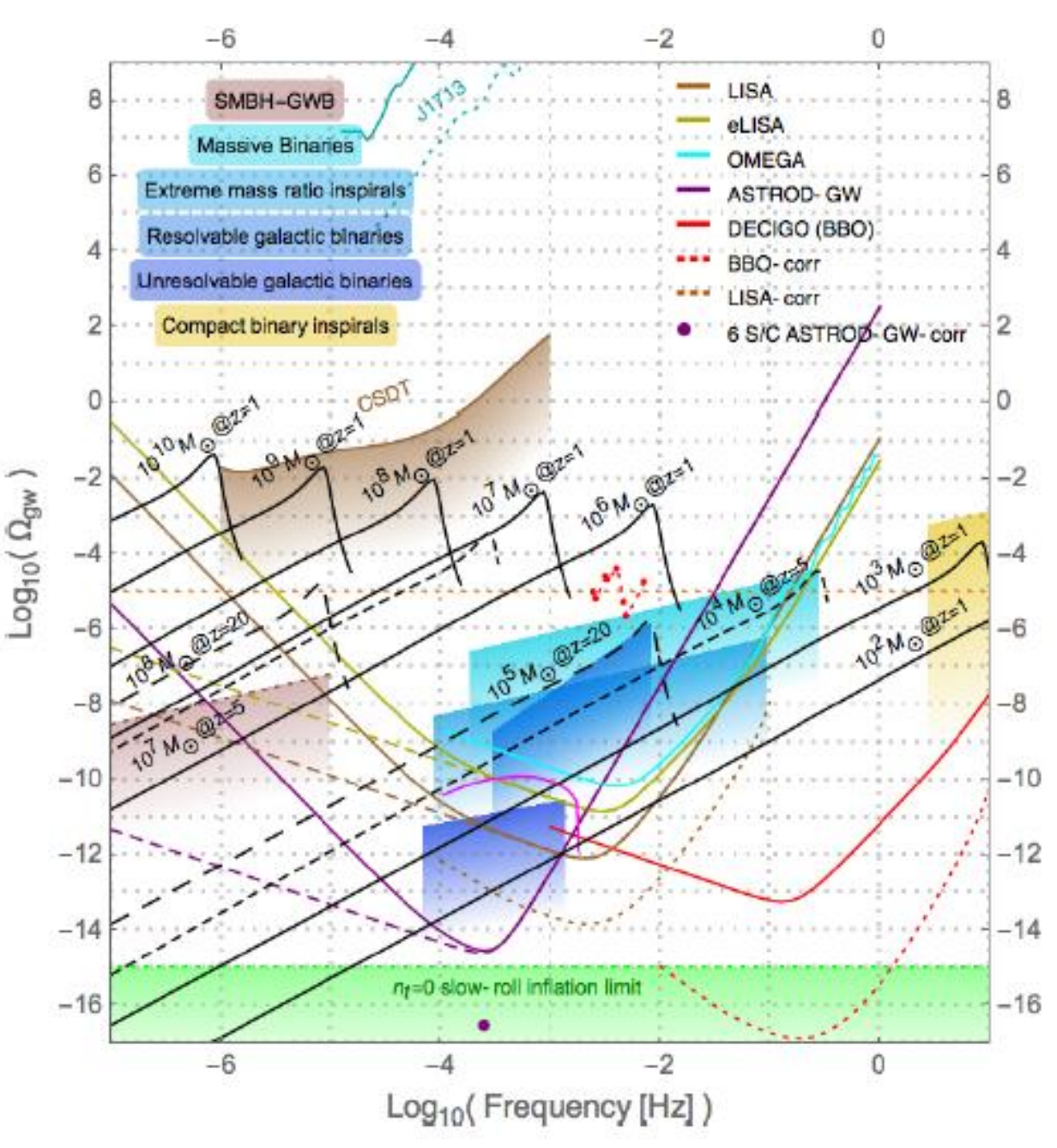
SMBH-GWB
Massive Binaries
Extreme mass ratio inspirals
Resolvable galactic binaries
Unresolvable galactic binaries
Compact binary inspirals
LISA
eLISA
OMEGA
ASTROD- GW
DECIGO (BBO)
BBO- corr
LISA- corr
6 S/C ASTROD- GW- corr
J1713
CSDT
$10^{10}M_\odot$@z=1
$10^{9}M_\odot$@z=1
$10^{8}M_\odot$@z=1
$10^{8}M_\odot$@z=20
$10^{7}M_\odot$@z=1
$10^{7}M_\odot$@z=5
$10^{6}M_\odot$@z=1
$10^{5}M_\odot$@z=20
$10^{4}M_\odot$@z=5
$10^{3}M_\odot$@z=1
$10^{2}M_\odot$@z=1
n_t=0 slow- roll inflation limit
$\mathrm{Log}_{10}(\Omega_{gw})$
Log_{10}(Frequency [Hz])

Massive Black Hole Systems: Massive BH Mergers & Extreme Mass Ratio Mergers (EMRIs)

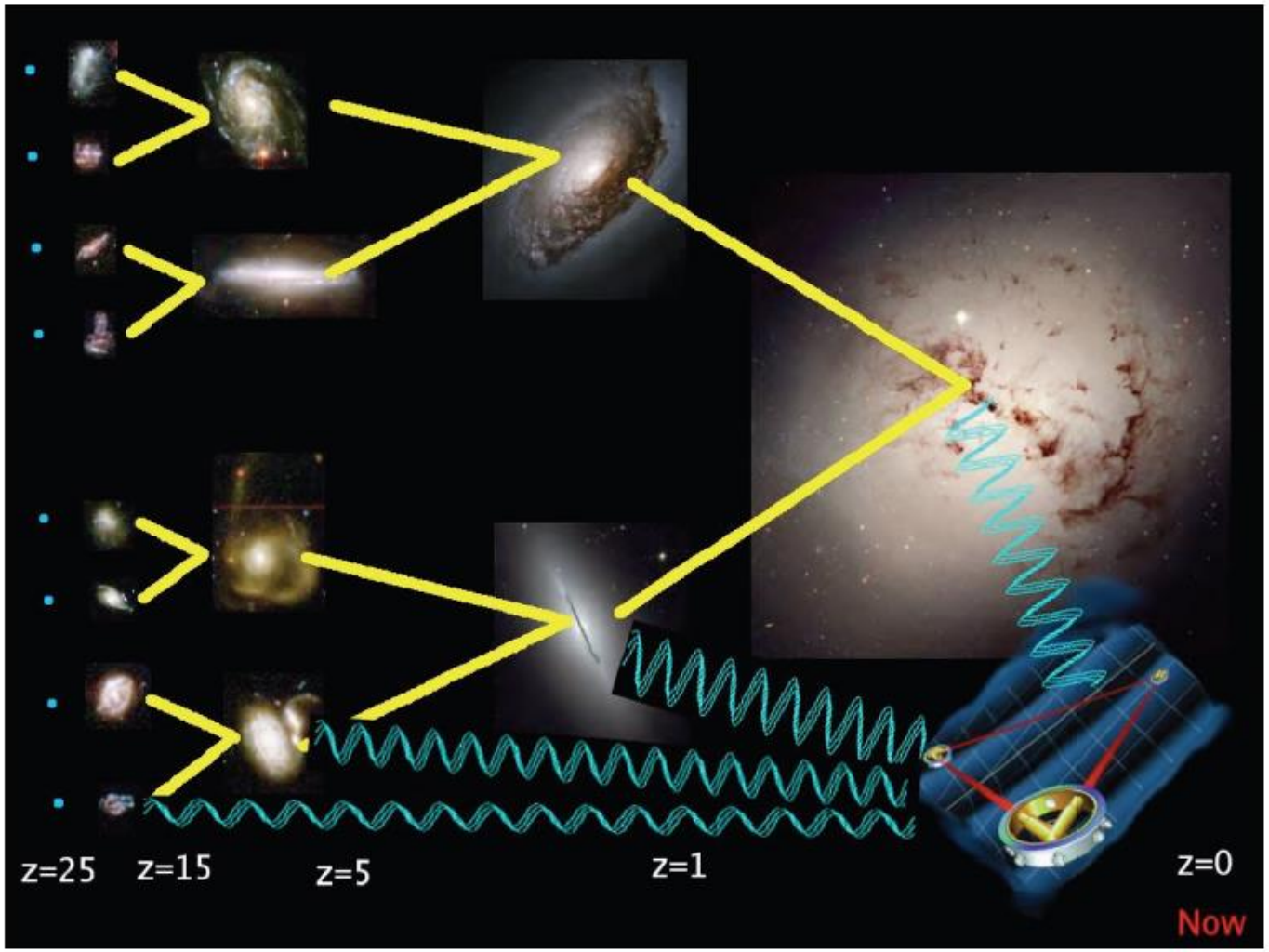

Scientific Goals

1. Massive black holes and their co-evolution with galaxies -- both (i) background, and (ii) individual sources with expected rate of 10 to 1000 per year with good angular resolution
2. Extreme mass ratio inspirals (EMRIs) – a few tens to 100 per year
3. Testing relativistic gravity – including testing strong-field gravity, precision probing of Kerr spacetime and measuring/constraining the mass of graviton
4. Dark energy and cosmology – Space GW detectors observing MBHB inspirals and EMRIs are good probes to determine the luminosity distances. Hence with better precision in angular determination for identification of electromagnetic counterparts,
5. Compact binaries are ideal to probe dark energy and cosmology
6. Relic GWs – 6 S/C formation (2 sets of 3 S/C formations) is ideal for this purpose

ASTROD-GW Orbit Design

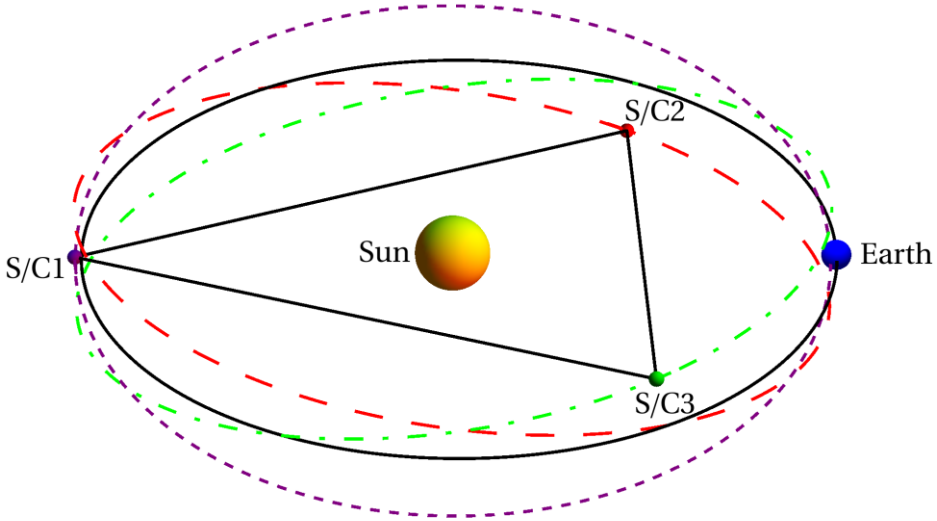

The inclined orbit configuratic

$$x = a\cos\varphi = a\cos(\omega t + \varphi_0); \quad y = a\sin\varphi = a\sin(\omega t + \varphi_0); \quad z = 0$$

Let us transform this orbit actively into an orbit with inclination, and with the intersection of the orbit plane and xy-plane at the line $\varphi = \Phi_0$ in the xy-plane. The

For the three orbits with inclination λ (in radian), we choose:

$$\text{S/C I}: \Phi_0(\text{I}) = 270^\circ, \quad \varphi_0(\text{I}) = 0^\circ,$$

$$\text{S/C II}: \Phi_0(\text{II}) = 150^\circ, \quad \varphi_0(\text{II}) = 120^\circ,$$

The normalized unit normal vector $\underline{n}$ is then .

$$\underline{n} = [\sin^2\lambda + (1-\xi/2)^2]^{1/2} \begin{bmatrix} -\sin\lambda\cos 2\omega t \\ -\sin\lambda\sin 2\omega t \\ (1-\xi/2) \end{bmatrix}$$

Orbit Design II

- With equations (4)-(6), the arm lengths are calculated to be

$$|\boldsymbol{V}_{\text{II-I}}| = 3^{1/2} a \left[\left(1 - \xi/2\right)^2 + \sin^2\lambda \sin^2\left(\omega t - 60^\circ\right) \right]^{1/2},$$

$$|\boldsymbol{V}_{\text{III-II}}| = 3^{1/2} a \left[\left(1 - \xi/2\right)^2 + \sin^2\lambda \sin^2\left(\omega t\right) \right]^{1/2},$$

$$|\boldsymbol{V}_{\text{I-III}}| = 3^{1/2} a \left[\left(1 - \xi/2\right)^2 + \sin^2\lambda \sin^2\left(\omega t + 60^\circ\right) \right]^{1/2}.$$

- The fractional arm length variation is within $\pm$ (1/2) $\sin^2\lambda$, e.g. $\pm 0.76 \times 10^{-4}$ for $\lambda = 1^\circ$. The Doppler velocity (line-of-sight velocity) between two spacecrafts, e.g. S/C II and S/C III is

$$\frac{\mathrm{d}|\boldsymbol{V}_{\text{III-II}}|}{\mathrm{d}t} = (3^{1/2}/2) a\omega \sin^2\lambda \sin\left(2\omega t\right) \left[\left(1 - \xi/2\right)^2 + \sin^2\lambda \sin^2\left(\omega t\right) \right]^{-1/2}.$$

- From this equation the line-of-sight Doppler velocity is less than $(3^{1/2}/2)\, a\omega \sin^2\lambda$ $(1 + O(\lambda^2))$.

Now consider orbit configuration with inclination $\lambda = 1°$. We start with the same initial conditions at noon, June 21, 2025 (JD2460848.0) as those in Refs. 64 and

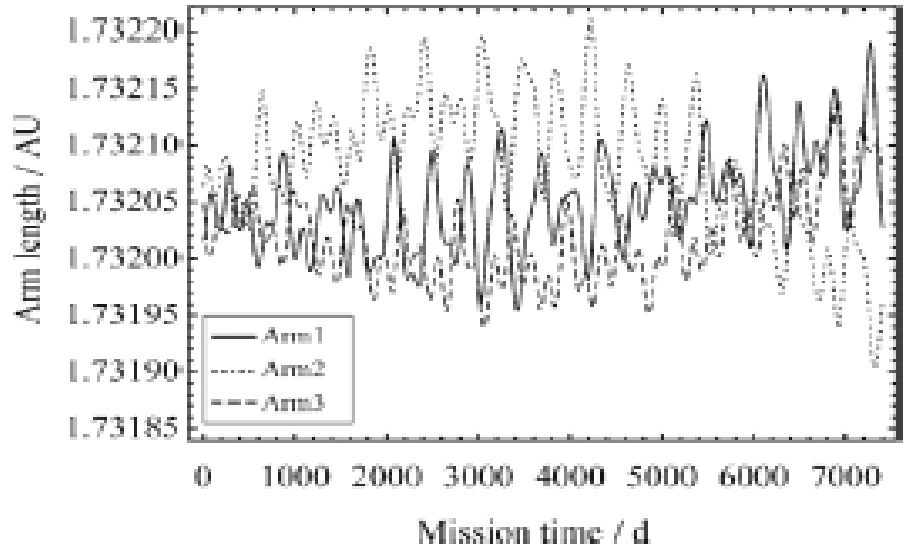

(a)

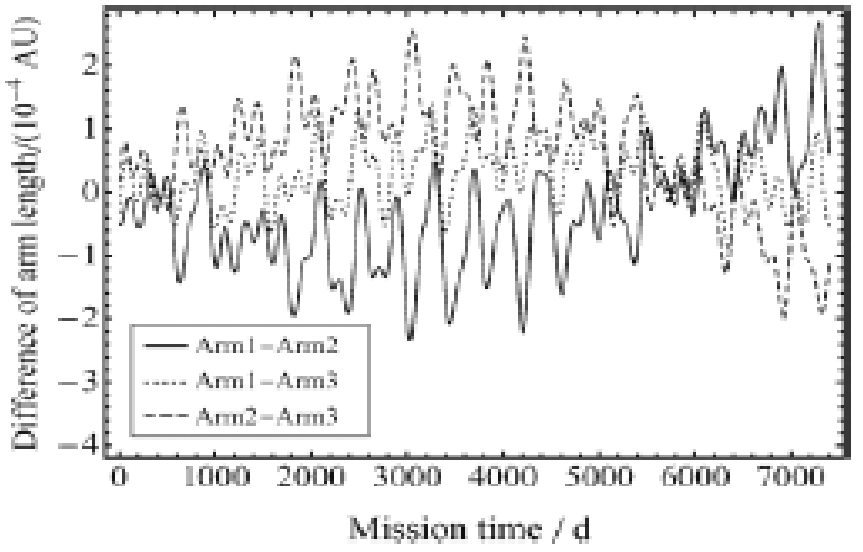

(b)

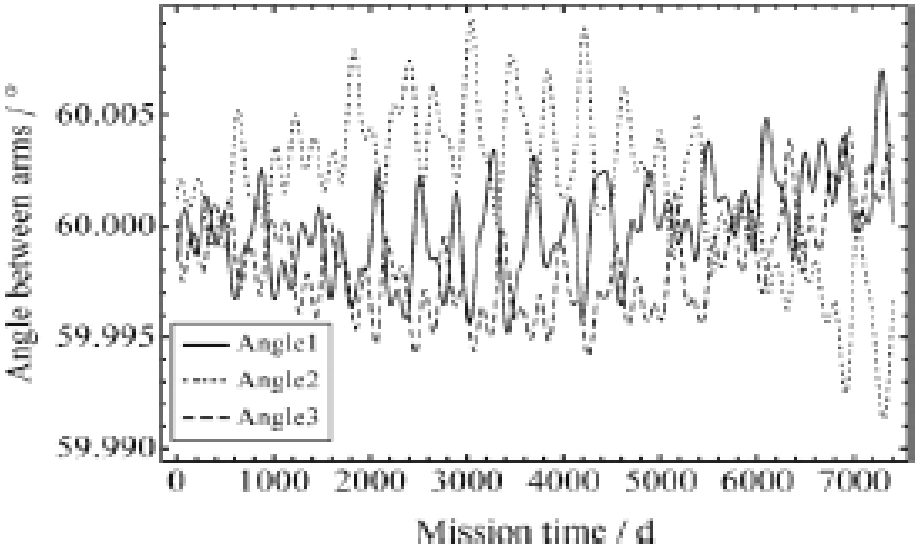

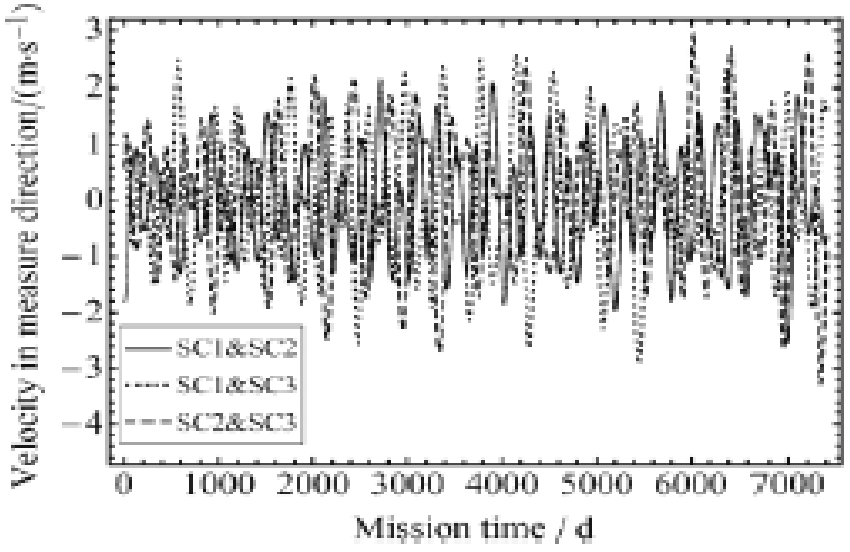

Arm length and Arm length difference

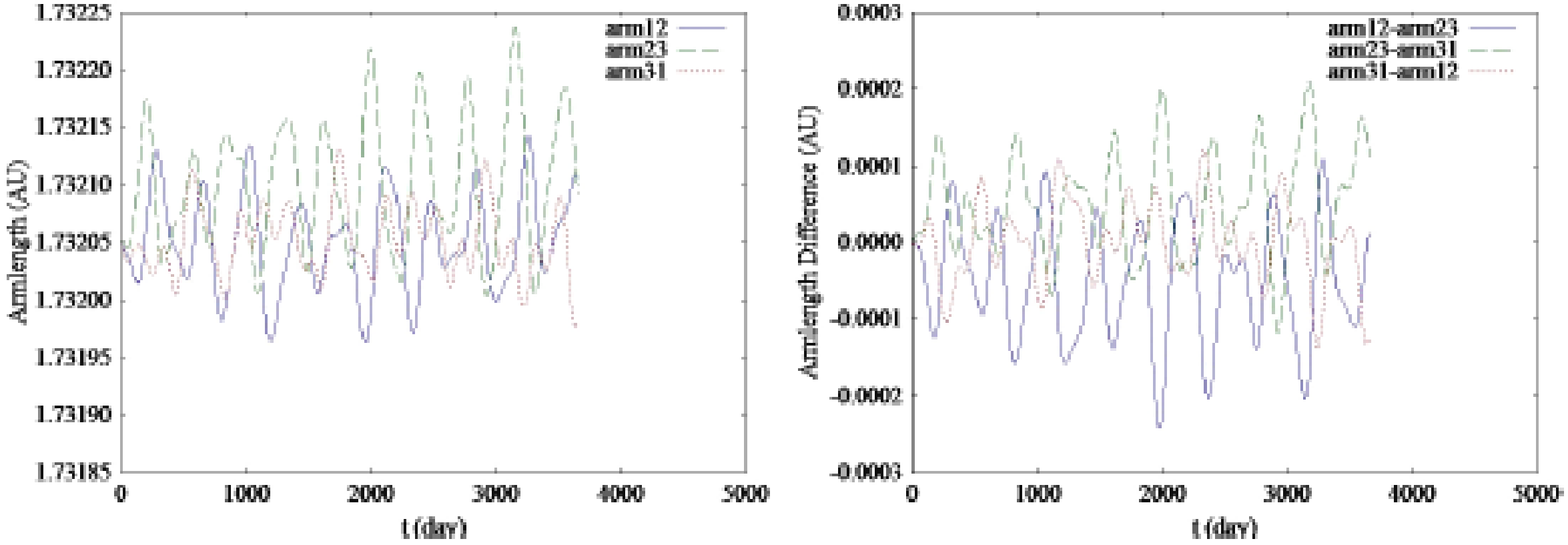

Fig. 7. Arm lengths (right) and arm length differences (left) for the case of 1° inclination after adjustment of initial velocity of S/C 1. Initial time is at noon, June 21, 2025 (JD2460848.0).

Deployment

Table 1. Estimated delta-V and propellant mass ratio for solar transfer of S/C.

S/C (destination)	Transfer orbit	Transfer time	Solar transfer delta-V after injection from earth orbit to solar transfer orbit	Solar transfer propellant mass ratio (Isp = 320 s)
1 (near L3)	Venus flyby transfer	1.3–1.5 yr	2.2–2.5 km/s	0.50–0.55
2 (near L4)	Inner Hohmann, 2 revolutions	1.833 yr	0.903 km/s	0.250
3 (near L5)	Outer Hohmann, 1 revolution	1.167 yr	1.422 km/s	0.365

Examples of Time Delay Interferometry TDI

(i) Unequal arm Michelson TDI configuration:

$$\text{Path 1: S/C 1} \to \text{S/C 2} \to \text{S/C 1} \to \text{S/C 3} \to \text{S/C 1},$$

$$\text{Path 2: S/C 1} \to \text{S/C 3} \to \text{S/C 1} \to \text{S/C 2} \to \text{S/C 1}.$$

(ii) Sagnac TDI configuration:

$$\text{Path 1: S/C 1} \to \text{S/C 2} \to \text{S/C 3} \to \text{S/C 1},$$

$$\text{Path 2: S/C 1} \to \text{S/C 3} \to \text{S/C 2} \to \text{S/C 1}.$$

X and Sagnac TDI

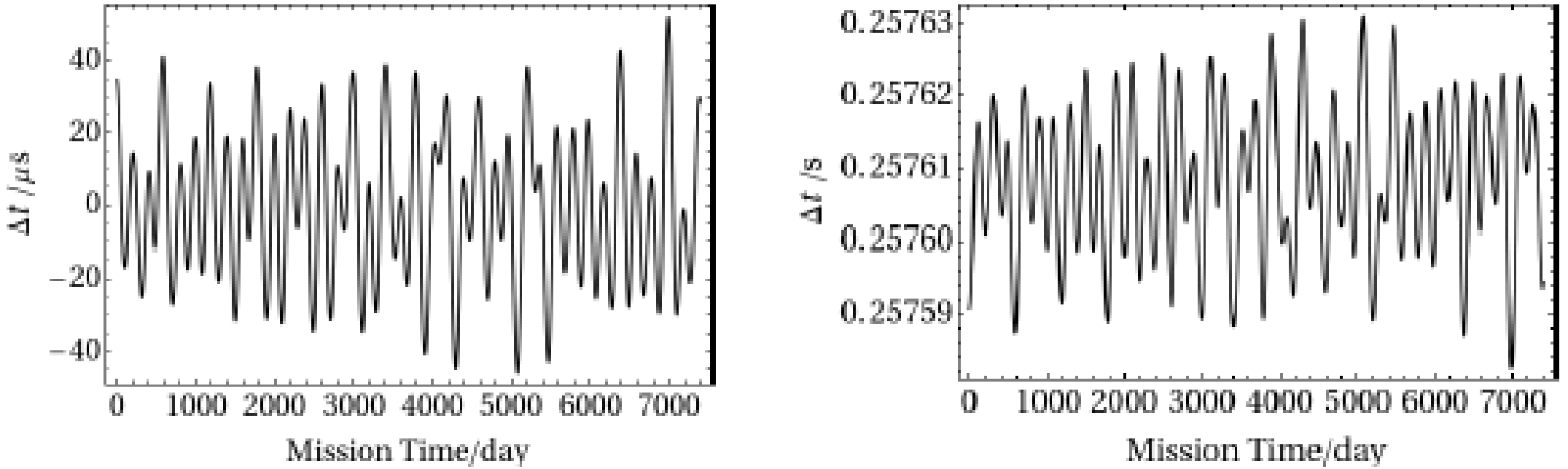

Fig. 8. The path length difference of two optical paths of ASTROD-GW for (a) unequal-arm Michelson TDI configuration (X observable) [a, b] and (b) Sagnac configuration.

Unequal-arm Michelson X, Y & Z TDIs and its sum X+Y+Z for new LISA

- 1999 Armstrong, Estabrook, Tinto, X, Y & Z TDIs X+Y+Z for LISA
- Vallisneri 2005 (U, P, E)
- Tinto & Dhurandhar review 2014

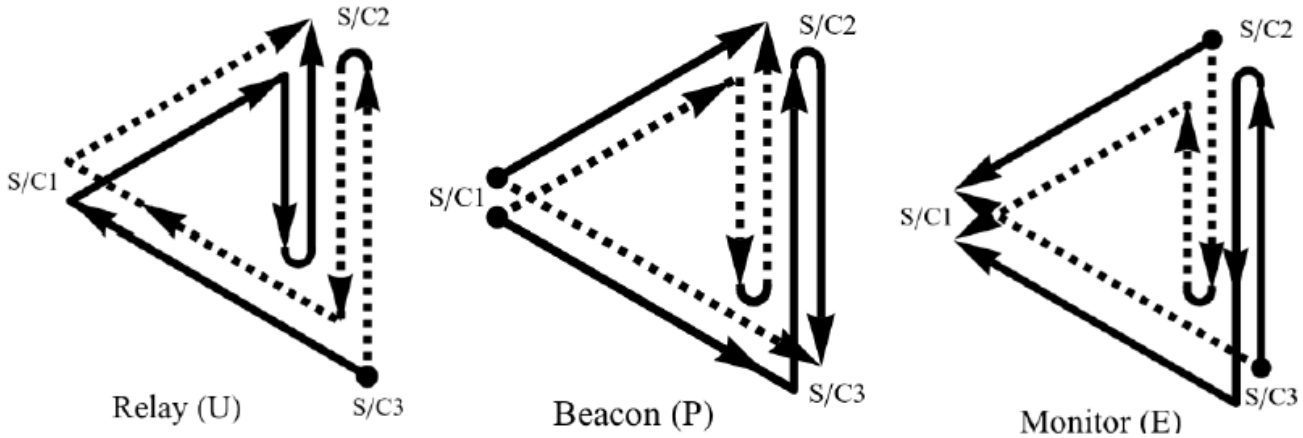

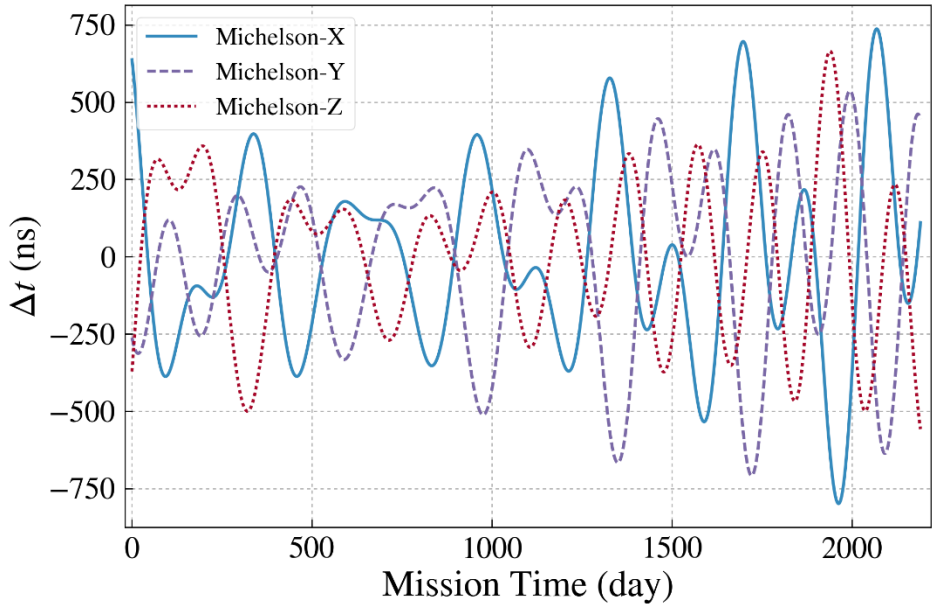

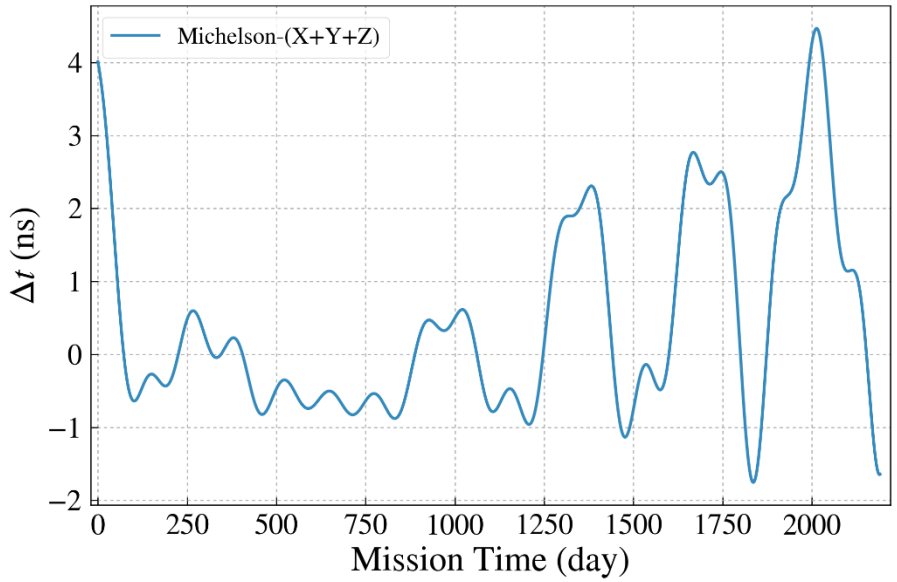

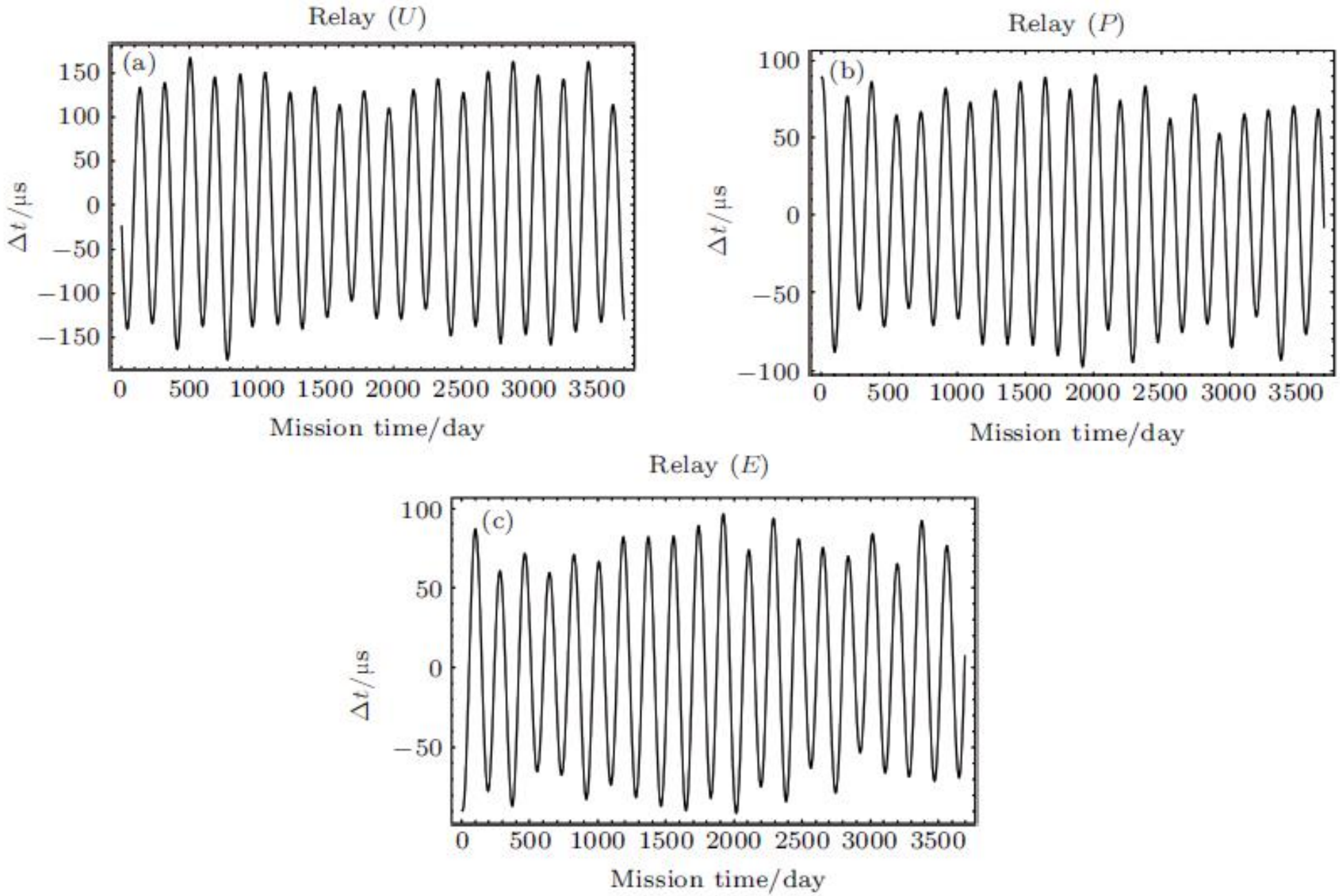

Fig. 6. Path length differences between two optical paths of the Relay-*U* (a), Beacon-*P* (b), and Monitor-*E* (c) TDI configurations for ASTROD-GW orbit formation with 1° inclination.

Table 4. Compilation of the rms path length differences of various first generation TDI configurations for various degrees of ASTROD-GW formation inclination (0°, 0.5°, 1°, 1.5°, 2°, 2.5°, and 3°) with respect to the ecliptic plane.

TDI configuration	ASTROD-GW TDI path difference ΔL						
	0°[μs]	0.5°[μs]	1°[μs]	1.5°[μs]	2.0°[μs]	2.5°[μs]	3.0°[μs]
Michelson-X	24	34	111	249	443	692	997
Michelson-Y	18	35	113	251	444	692	996
Michelson-Z	23	36	115	253	447	697	1002
Sagnac-α	257610	257590	257531	257432	257293	257115	256898
Sagnac-β	257608	257588	257529	257431	257294	257118	256902
Sagnac-γ	257607	257588	257530	257432	257297	257122	256909
Relay-U	17	31	100	219	387	602	866
Relay-V	18	29	96	216	383	598	861
Relay-W	21	30	98	217	385	602	867
Beacon-P	12	17	56	125	222	346	499
Beacon-Q	9	18	57	136	222	346	498
Beacon-R	12	18	58	127	224	349	501
Monitor-E	12	17	56	125	222	346	499
Monitor-F	9	18	57	136	222	346	498
Monitor-G	12	18	58	127	224	349	501

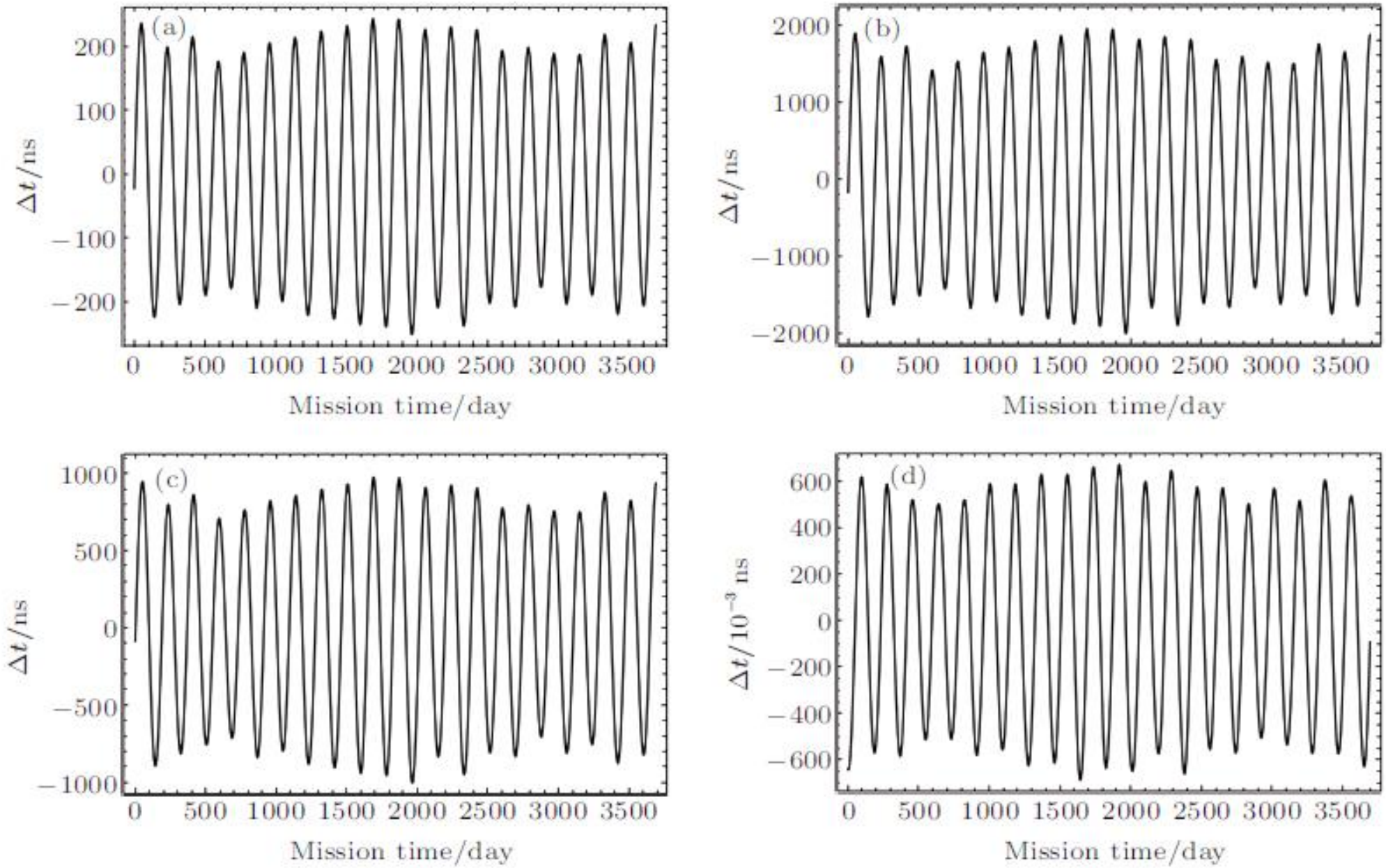

Fig. 7. Path length differences between two optical paths of second generation TDIs $n = 1$ and $n = 2$ TDI configurations for ASTROD-GW orbit formatic with 1° inclination. (a) $[ab, ba]$, (b) $[a^2b^2, b^2a^2]$, (c) $[abab, baba]$, (d) $[ab^2a, ba^2b]$.

Table 5. Compilation of the rms path length differences of various TDI configurations in the case of one interferometric detector with two arms (vertex at S/C1) for various degrees of ASTROD-GW formation inclination (0°, 0.5°, 1°, 1.5°, 2°, 2.5°, and 3°) with respect to the ecliptic plane. [Nominal ASTROD-GW arm length: 260 Gm].

TDI configuration		ASTROD-GW TDI path difference ΔL						
		0°[ns]	0.5°[ns]	1°[ns]	1.5°[ns]	2.0°[ns]	2.5°[ns]	3.0°[ns]
$n=1$	$[ab, ba]$	22	41	152	342	608	951	1370
	$[a^2b^2, b^2a^2]$	173	328	1209	2729	4862	7605	10957
$n=2$	$[abab, baba]$	87	164	605	1365	2431	3803	5479
	$[ab^2a, ba^2b]$	0.0536	0.112	0.417	0.942	1.68	2.63	3.78
	$[a^3b^3, b^3a^3]$	582	1106	4079	9208	16407	25667	36980
	$[a^2bab^2, b^2aba^2]$	453	860	3172	7162	12761	19964	28762
	$[a^2b^2ab, b^2a^2ba]$	323	615	2266	5116	9115	14260	20544
	$[a^2b^3a, b^2a^3b]$	194	369	1360	3070	5469	8556	12327
$n=3$	$[aba^2b^2, bab^2a^2]$	323	615	2266	5116	9115	14260	20545
	$[ababab, bababa]$	194	369	1360	3070	5469	8556	12327
	$[abab^2a, baba^2b]$	65	123	454	1024	1823	2852	4109
	$[ab^2a^2b, ba^2b^2a]$	65	123	454	1024	1823	2852	4109
	$[ab^2aba, ba^2bab]$	65	123	454	1024	1823	2852	4109
	$[ab^3a^2, ba^3b^2]$	194	369	1360	3070	5469	8556	12327

important issues for further studies in order to realize and sharpen our expectations

(i) Manipulating weak light.
(ii) Improvement of low-frequency acceleration noise.
(iii) Fourier spectrum of perturbations due to celestial bodies in the solar-system and precision needed to know the positions of solar-system bodies in order to separate this spectrum from GW spectrum.
(iv) Further studies in optimizing deployment delta-V and propellant ratio (common problem to DECIGO/BBO and some other future missions to come).
(v) Optimizing the inclination angle of the ASTROD-GW constellation.
(vi) Extraction of GW signals based on precise numerical orbits.
(vii) Further studies in the angular resolution of GW sources of ASTROD-GW.
(viii) Separation of weak lensing effects from GW signals.


Thank
You